On the theory of sea-floor conductivity mapping using transient electromagnetic systems

S. J. Cheesman*, R. N. Edwards*, and A. D. Chave‡

ABSTRACT

The electrical conductivity of the sea floor is usually much less than that of the seawater above it. A theoretical study of the transient step-on responses of some common controlled-source, electromagnetic systems to adjoining conductive half-spaces shows that two systems, the horizontal, in-line, electric dipole-dipole and horizontal, coaxial, magnetic dipole-dipole, are capable of accurately measuring the relatively low conductivity of the sea floor in the presence of seawater. For these systems, the position in time of the initial transient is indicative of the conductivity of the sea floor, while at distinctly later times, a second characteristic of the transient is a measure of the seawater conductivity. The diagnostic separation in time between the two parts of the transient response does not occur for many other systems, including several systems commonly used for exploration on land. A change in the conductivity of the sea floor produces a minor perturbation in what is essentially a seawater response.

Some transient responses which could be observed with a practical, deep-towed coaxial magnetic dipole-dipole system located near the sea floor are those for the half-space, the layer over a conductive or resistive basement, and the half-space with an intermediate resistive zone. The system response to two adjoining half-spaces, representing seawater and sea floor, respectively, is derived analytically. The solution is valid for all time, provided the conductivity ratio is greater than about ten, or less than about one-tenth. The analytic theory confirms the validity of numerical evaluations of closed-form solutions to these layered-earth models.

A lateral conductor such as a vertical, infinite, conductive dike outcropping at the sea floor delays the arrival of the initial crustal transient response. The delay varies linearly with the conductance of the dike. This suggests that time delay could be inverted directly to give a measure of the anomalous integrated conductance of the sea floor both between and in the vicinity of the transmitter and the receiver dipoles.

INTRODUCTION

Over three-fifths of the Earth's surface is covered by the oceans and shallow seas. Even though petroleum is produced from huge deposits on the continental shelf, this immense area represents a largely unexplored and unexploited resource base. Until recently, little interest was shown in the ocean-floor environment, which, with the possible exception of manganese nodules, was assumed to be essentially barren. However, the recent discovery of polymetallic sulfide mineralization on the crest of the East Pacific rise (Hekinian et al., 1980), the Galapogos ridge (Malahoff, 1982), and the Juan de Fuca plate (Normark et al., 1983) has spurred interest in the possibility of deep-sea mining. The present deposits were located visually with submersibles and mapped acoustically with instrument packages such as SEABEAM (Ballard and Francheteau, 1982), which can determine bathymetry with high precision. While these methods have been able to examine surficial geology, they cannot adequately assess the extent of the deposits and the structure of the regional geology in which they are found. Sea-floor conductivity mapping using the electromagnetic (EM) method is one of the few geophysical tools suitable for this purpose. On land, EM mapping is routinely carried out from the air. A simple apparent resistivity map systematically produced in one pass from airborne data can detect boundaries between different types of rock and directly identify local 3-D targets, such as base-metal mineral deposits, which are

much more conductive than the host rocks in which they are found. It is our aim to produce a similar mapping tool for the sea floor that operates on a similar scale, on the order of a hundred meters. Some of the theoretical problems associated with the design of such a system are described here.

The method is certainly not limited to locating mineral deposits. It also has applications as a tool in the detection of subsea permafrost (a resistive zone relative to its environment) and as a supplementary technique to seismic in offshore oil exploration. Physical properties such as porosity, bulk density, water content, and compressional wave velocity may be estimated from a profile of the electrical conductivity with depth (Nobes et al., 1986).

The elementary theory of the frequency response of a crustal layer beneath a more conductive seawater has been described by Bannister (1968), Chave and Cox (1982), Coggon and Morrison (1970), Edwards et al. (1981) and Kaufman and Keller (1983). The rationale for a broadband EM system has been set out by Edwards and Chave (1986), who computed the response of a crustal half-space beneath a more conductive half-space representing seawater, to a transient electric dipole-dipole system. In describing their observations physically, we use the concept of the "smoke ring" (Nabighian, 1979). Induced-current smoke rings of the EM field excited by an event in the transmitter diffuse outward through both the seawater and the less conductive sea floor. The rate of diffusion through a medium is inversely proportional to the conductivity of the medium, so that in the most common instance (a resistive sea bed), the EM field diffusing through the sea floor reaches the receiver first. The signal diffusing through the seawater arrives later, and ultimately the measured field approaches the static limit. Edwards and Chave (1986) showed
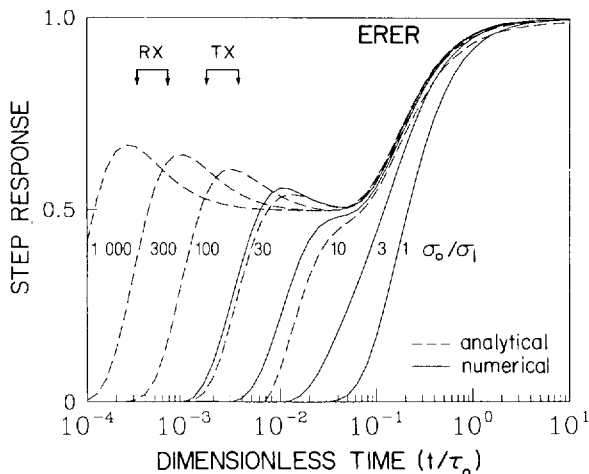

FIG. 1. The step-on response for the coaxial electric dipole-dipole system (ERER) evaluated analytically from equation (38) and numerically from the frequency-domain equations (2) and (3) in Edwards and Chave (1986) for a range of values of the conductivity ratio between the seawater and the sea floor. The initial step to about three-quarters of the static limit occurs at different times and is due to propagation in the sea floor. The secondary step at constant time is due to propagation in the seawater. The time axis is normalized by dividing true time by the characteristic diffusion time in the sea water τ_0. [For a definition of τ, see equation (18).] The response axis is normalized by dividing by the response at late time.

that the transient coaxial electric dipole-dipole (ERER) system is particularly useful for determining sea-floor conductivity. The normalized step-on response of this system is plotted in Figure 1 for a range of values of the conductivity ratio between the seawater and the sea floor. The initial step to three-quarters of the static limit is due to propagation in the sea floor; the second step at a constant, later time is due to propagation in the sea. Clearly, the position in time of the initial rise in the sea-floor response is a direct measure of the sea-floor conductivity and, for many practical values of the conductivity ratio, the separation in time between the two parts of the transient response, and hence the resolution of sea floor conductivity, is substantial.

The theoretical curves computed by Edwards and Chave are displayed in the time domain. A similar separation of sea-floor and seawater effects is also observed in the frequency domain. Electing to display results in the time domain reduces the number of curves by a factor of two, because in the frequency domain, graphs of both amplitude and phase are required. From the point of view of physics, the two domains are equivalent, and perfect data collected in one domain can be transformed into the other using Fourier's theorem. However, in practice simple measurements in the two domains to the same degree of accuracy do not necessarily provide the same information. For example, the diagnostic late-time response of a finite conductor is observed directly in time, but the same information cannot be gleaned from frequency-domain data unless accurate gradients of the amplitude response are known at low frequency. A good analogy is found in the magnetotelluric method. Theoretically, it is possible to transform apparent resistivity data into phase data, so it appears that measuring both would be redundant. Yet most protagonists of this method are quick to point out that phase data can sometimes yield additional information because the experimental error on a phase measurement is often much smaller than the corresponding error on a phase datum derived from an apparent resistivity data set with its experimental error. The relative merits of broadband frequency and broadband transient systems have been discussed extensively in GEOPHYSICS; they depend on theoretical, statistical, and practical factors. In reality, the choice of a frequency-domain system over a transient system, or vice versa, could well be academic, since both systems require transmission of a continuous, broadband signal and reception with a broadband detector. The response of the earth is a deconvolution of the received signal with the transmitted signal combined with the system response; ultimately it is the choice of frequency-domain or time-domain formulations of this deconvolution process which distinguishes the time from the frequency domain character.

The question now arises, "What other EM systems show similar characteristics when operated in the marine environment?" The theory of using EM systems to determine the electrical resistivity of continental material is reasonably well understood and documented (Hohmann and Ward, 1986; Spies and Frischknecht, 1986). Some of the more common systems that have been used with success on land, particularly in a layered-earth environment, are illustrated in Figure 2. The coplanar magnetic dipole (HZHZ) system and the coaxial magnetic dipole (HRHR) system can be grouped together as far as the physics is concerned. They both generate only hori-

zontal current flow in a 1-D earth, and they are both relatively insensitive to thin horizontal resistive zones. The ERER system, which generates both vertical and horizontal current flow, is preferred when such zones have to be mapped. The thin resistive layer is detected by the deflection in the electric field (and current) caused by electric charge build-up. A fifth system, in which the transmitter is a horizontal electric dipole and the receiver is a vertical magnetic dipole (EPHIHZ), is also used. Although both modes of current flow are generated by the electric dipole transmitter, the receiver sees only the magnetic field of the horizontal current flow so that interpretation of data obtained with this system follows the same path as for HZHZ or HRHR.

The grouping of these systems when operated on the sea floor is fundamentally different. With the present method, the systems are buried inside a conductive medium; preconceptions based on their terrestrial use can be quite misleading. Whereas HZHZ still generates only horizontal current flow, both ERER and HRHR generate and receive both modes. Furthermore, the secondary EM fields due to induction in the crustal material are measured at or near the surface of a relatively good conductor. Consequently, a system such as HZHZ, which measures a component of a field which vanishes at the surface of a good conductor, is unlikely to produce data sensitive to a resistive sea floor. The most useful characteristic for inferring the suitability of a system for use on the sea floor from its behavior when used on land is the initial behavior of its step-on response. At time zero, there must be a jump from zero field to a finite value; for example, the ERER response jumps instantaneously (actually on a time scale based on the speed of light) to one-half the late-time value when used at the surface of a uniform earth. Replacing the air by a weakly conductive second half-space, in this case the sea floor, delays and broadens this initial rise. The HRHR system has a similar characteristic, but the instantaneous response is twice the late-time free-space static limit for either a resistive or a conductive sea floor. From a practical point of view, the field amplitude and delay times associated with the system on the 100 m scale are similar to those currently employed by commercial, land-based systems. Consequently, the construction of such a system poses no severe technical difficulties, and it is principally for this reason that it was chosen for detailed study.

The response of the system at the boundary of two half-spaces is calculated analytically for cases with a high conductivity contrast and numerically for cases with a low contrast. The responses of HZHZ and EPHIHZ, which have previously been suggested as possible ocean-bottom resistivity profiling systems, are also examined. They are shown to be unsuitable when the sea floor is resistive, because they do not show the separation of the signals from seawater and the sea floor. Only in the rare circumstance of the sea floor being locally more conductive than seawater are these systems sensitive to the conductivity of the sea floor.

The HRHR system response is investigated further by determining the step-on response to several other simple geologic models: the resistive layer, the resistive and conductive basements, and the vertical conductive dike. Finally, estimates of two possible sources of error associated with use of a practical system are obtained. Errors due to imperfect positioning are estimated by raising the receiver off the sea floor, while errors due to misalignment of the transmitter are estimated by deter-

mining the radial magnetic field produced by a vertical transient magnetic dipole transmitter (HZHR).

THE TRANSIENT RESPONSE OF TWO HALF-SPACES IN CONTACT

The coaxial magnetic dipole-dipole system (HRHR)

The coaxial horizontal magnetic dipole-dipole system shown in Figure 3 consists of a transmitter (TX) and a receiver (RX), separated by a horizontal distance p. The system is located in an upper half-space of conductivity σ_0 at a height h above the horizontal boundary with a lower half-space of conductivity σ_1. Dey and Ward (1970) derive a solution for the
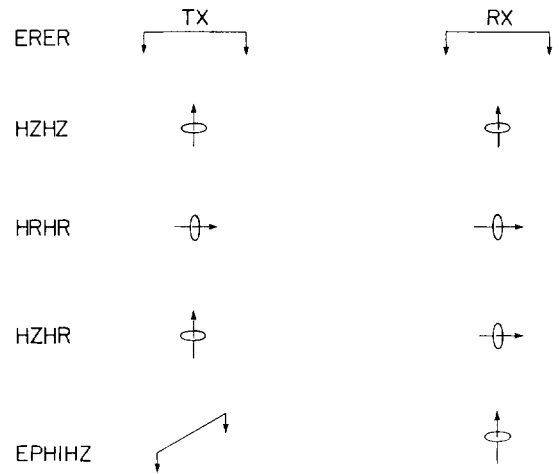

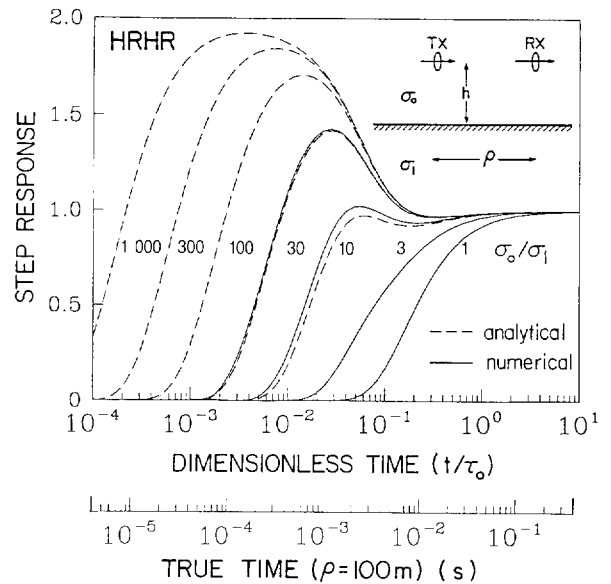FIG. 2. Some possible transmitter and receiver configurations for a sea-floor EM system.

FIG. 3. The normalized step-on response for the coaxial magnetic dipole-dipole system (HRHR) computed analytically from equation (22) and numerically from the frequency-domain equations (3) and (4) for a range of values of the conductivity ratio α. The second time axis gives the true response time for a sea-floor system $\sigma_0 = 3.1$ S/m with a separation $\rho = 100$ m.

general layered-earth response of the system. Subject to the approximation that the magnetic effects of displacement currents can be neglected, the magnetic field at the receiver, for a transmitter of magnetic moment $me^{i\omega t}$, is

$$\frac{4\pi}{m} H_\rho(\omega) = -k_0^2 \int_0^\infty \left[\frac{\lambda}{u_0} + A_1(\lambda) \right] J_0(\lambda\rho) e^{-u_0 h} \, d\lambda$$

$$+ \frac{1}{\rho} \int_0^\infty \left[\frac{\lambda}{u_0} + R(\lambda) \right] \lambda J_1(\lambda\rho) e^{-u_0 h} \, d\lambda$$

$$- \int_0^\infty \left[\frac{\lambda}{u_0} + R(\lambda) \right] \lambda^2 J_0(\lambda\rho) e^{-u_0 h} \, d\lambda, \qquad (1)$$

where

$$A_1(\lambda) = \frac{\lambda}{u_0} R_{TM}(\lambda)$$

and

$$R(\lambda) = A_1(\lambda) - \frac{u_0}{\lambda} (R_{1M} + R_{PM}),$$

and where in the ith medium $u_i^2 = \lambda^2 + k_i^2$ and $k_i^2 = i\omega\mu_0\sigma_i$. The R_{TM} and R_{PM} terms are the reflection coefficients for the independent toroidal (TM) and poloidal (PM) modes, characterized by the absence of a vertical component of the magnetic and electric fields, respectively (Chave, 1984).

Assuming zero initial conditions, expression (1) with the product $i\omega$ replaced by the complex Laplace variable s is in the form of a Laplace transform. The value of the magnetic field $H_\rho(s)$ at the boundary is determined by taking the limit as h approaches zero. It is of the form

$$H_\rho(s) = \frac{m(s)}{4\pi} \left[F_{TM}(s) + F_{PM}(s) \right], \qquad (2)$$

where $m(s)$ is the Laplace transform of the source-current dipole moment. The functions F_{TM} and F_{PM} are given by

$$F_{TM}(s) = -\int_0^\infty (R_{TM} + 1) \frac{k_0^2}{u_0 \rho} J_1(\lambda\rho) \, d\lambda, \qquad (3)$$

and

$$F_{PM}(s) = \int_0^\infty (R_{PM} - 1) \left[u_0 \lambda J_0(\lambda\rho) - \frac{u_0}{\rho} J_1(\lambda\rho) \right] d\lambda. \qquad (4)$$

The modal reflection coefficients for our double half-space model are

$$R_{1M} = \frac{u_0 \sigma_1 - u_1 \sigma_0}{u_0 \sigma_1 + u_1 \sigma_0}, \qquad (5)$$

and

$$R_{PM} = \frac{u_0 - u_1}{u_0 + u_1}. \qquad (6)$$

Since both the transmitter and the receiver lie on the interface between the two half-spaces, equations (3) and (4) may be written in forms which, by symmetry, are invariant when the half-space indices are interchanged. The expressions become

$$F_{TM}(s) = -\frac{2\mu_0 \sigma_0 \sigma_1 s}{\rho} \int_0^\infty \frac{J_1(\lambda\rho)}{u_0 \sigma_1 + u_1 \sigma_0} \, d\lambda, \qquad (7)$$

and

$$F_{PM}(s) = -\frac{\partial}{\partial\rho} \int_0^\infty \frac{2u_0 u_1}{u_0 + u_1} J_1(\lambda\rho) \, d\lambda. \qquad (8)$$

Equation (7) cannot be evaluated analytically because of the presence of multiple branch cuts. However, it may be approximated for certain cases. The conductivity σ_0 of the upper half-space, i.e., the sea, is usually significantly greater than the conductivity σ_1 of the lower half-space, the crust, so that we may expand equation (7) in powers of $u_0\sigma_1/u_1\sigma_0$ and drop second-order and higher terms. A complementary approximation may be made when the sea floor is relatively conductive ($\sigma_1 \gg \sigma_0$). It is still not possible to evaluate terms with u in the numerator because of the branch cuts, so a second assumption is made: In the range of values of λ where the significant contribution to the total integral is made, $\lambda^2 \ll |s\mu_0\sigma_0|$, so that u_0 may be approximated by k_0. This approximation is valid in the midfield ($|s\mu_0\sigma_0| \gg 1/\rho^2 \gg |s\mu_0\sigma_1|$) and in the far field ($|s\mu_0\sigma_1| \gg 1/\rho^2$). In the near field ($1/\rho^2 \gg |s\mu_0\sigma_0|$), where the greatest discrepancy is introduced, the approximation's inherent error may be shown to be at most of order σ_1/σ_0. Equation (7) under this approximation becomes

$$F_{TM}(s) = -\frac{2k_1^2}{\rho} \int_0^\infty \frac{1}{u_1} \left[1 - \frac{k_0\sigma_1}{u_1\sigma_0} \right] J_1(\lambda\rho) \, d\lambda. \qquad (9)$$

The first and second terms in equation (9) may be evaluated using the standard integrals

$$\int_0^\infty \frac{J_1(\lambda\rho)}{u} \, d\lambda = \frac{1}{k\rho} \left[1 - \exp(-k\rho) \right], \qquad (10)$$

and

$$\int_0^\infty \frac{J_1(\lambda\rho)}{u^2} \, d\lambda = \frac{1}{k^2\rho} \left[1 - k\rho K_1(k\rho) \right], \qquad (11)$$

where equation (11) may be derived by the differentiation of Mehler's integral (Watson, 1966). The expression for the TM mode then becomes

$$\frac{\rho^3}{2} F_{TM}(s) = \frac{\sigma_1}{\sigma_0} k_0 \rho - k_1\rho + k_1\rho \exp(-k_1\rho)$$

$$- \sqrt{\frac{\sigma_1}{\sigma_0}} k_1^2\rho^2 K_1(k_1\rho). \qquad (12)$$

Equation (8) for the PM mode may be evaluated by multiplying the numerator and the denominator by $u_0 - u_1$. This yields the exact expression

$$F_{PM}(s) = \frac{2}{k_0^2 - k_1^2} \frac{\partial}{\partial\rho} \left[\int_0^\infty (u_0 - u_1)\lambda^2 J_1(\lambda\rho) \, d\lambda \right.$$

$$\left. + \int_0^\infty (k_1^2 u_0 - k_0^2 u_1) J_1(\lambda\rho) \, d\lambda \right], \qquad (13)$$

which is evaluated using the standard integrals

$$\int_0^\infty u J_1(\lambda\rho) \, d\lambda = \frac{1}{\rho^2} \left[k\rho + \exp(-k\rho) \right], \qquad (14)$$

and

$$\int_0^\infty u\lambda^2 J_1(\lambda\rho)\,d\lambda = \frac{-1}{\rho^4}\left(k^2\rho^2 + 3k\rho + 3\right)\exp(-k\rho), \quad (15)$$

to give the following expression:

$$\begin{aligned}
F_{PM}(s) = \frac{2}{(k_0^2 - k_1^2)\rho^5}\Big\{ & k_0 k_1(k_0 - k_1)\rho^3 \\
& - \Big[k_0(k_1^2 - k_0^2)\rho^3 + (2k_1^2 - 5k_0^2)\rho^2 \\
& \quad - 12k_0\rho - 12 \Big]\exp(-k_0\rho) \\
& + \Big[k_1(k_0^2 - k_1^2)\rho^3 + (2k_0^2 - 5k_1^2)\rho^2 \\
& \quad - 12k_1\rho - 12 \Big]\exp(-k_1\rho)\Big\}.
\end{aligned} \quad (16)$$

Both $F_{PM}(s)$ and $F_{TM}(s)$ contain terms without exponential behavior, which tend to infinity for large values of s, or equivalently in the time domain, as t approaches zero. In fact, the field must be zero for times smaller than ρ/c, where c is the speed of light. The $1/\rho^2$ terms in the PM mode must cancel those in the TM mode physically, but because of the approximation introduced in the evaluation of the TM mode, the cancellation is not exact. There are two satisfactory ways to resolve this problem. The first would be to replace the $\sigma_0/(\sigma_0 - \sigma_1)$ and $\sigma_1/(\sigma_0 - \sigma_1)$ terms in equation (16), the PM mode, with 1 and σ_1/σ_0, respectively. The second solution would be to do the reverse to equation (12), the TM mode, i.e., replace σ_1/σ_0 terms with $\sigma_1/(\sigma_0 - \sigma_1)$ and terms of order unity with $\sigma_0/(\sigma_0 - \sigma_1)$. The second method is preferable for two reasons. First, the exact nature of the PM solution is unaltered (the TM solution already has errors of order σ_1/σ_0). In addition, the property that the field at late times approaches the whole-space field is preserved: the first method would introduce an error in the late-time amplitude of order σ_1/σ_0. The TM mode found in equation (12) is thus multiplied by $\sigma_0/(\sigma_0 - \sigma_1)$, and the result is added to the PM mode equation (16). The physically unreasonable singular terms cancel, and the final expression for the magnetic field becomes

$$\begin{aligned}
H_\rho(s) = \frac{m(s)}{2\pi\rho^3(\tau_0 - \tau_1)s}\Big\{ & -\sqrt{\tau_0 s(\tau_1 s)^3}\,K_1(\sqrt{\tau_1 s}) \\
& - \Big[\sqrt{\tau_0 s}(\tau_1 - \tau_0)s + (2\tau_1 - 5\tau_0)s \\
& \quad - 12\sqrt{\tau_0 s} - 12 \Big]\exp(-\sqrt{\tau_0 s}) \\
& + \Big[\sqrt{\tau_1 s}(2\tau_0 - \tau_1)s + (2\tau_0 - 5\tau_1)s \\
& \quad - 12\sqrt{\tau_1 s} - 12 \Big]\exp(-\sqrt{\tau_1 s})\Big\},
\end{aligned} \quad (17)$$

where the EM diffusion time constant for the ith medium is

$$\tau_i = \mu_0 \sigma_i \rho^2. \quad (18)$$

The time constant increases with the square of the transmitter-receiver separation and with the given conductivity, as expected for a purely diffusive process.

Equation (17) may be inverted to the time domain if the Laplace transform $m(s)$ of the source current dipole moment is specified. A current I switched on at time $t = 0$ in a one-turn coil of area ΔA and held constant has the transform

$$m(s) = I\Delta A/s. \quad (19)$$

The relevant Laplace transforms are

$$\frac{1}{s^2}\exp(\sqrt{\tau s}) \Leftrightarrow \left(t + \frac{\tau}{2}\right)\text{erfc}\left(\sqrt{\frac{\tau}{4t}}\right) - \sqrt{\frac{\tau t}{\pi}}\exp\left(-\frac{\tau}{4t}\right),$$

$$\frac{1}{s^{3/2}}\exp(\sqrt{\tau s}) \Leftrightarrow \sqrt{\frac{4t}{\pi}}\exp\left(-\frac{\tau}{4t}\right) - \sqrt{\tau}\,\text{erfc}\left(\sqrt{\frac{\tau}{4t}}\right),$$

$$\frac{1}{s}\exp(\sqrt{\tau s}) \Leftrightarrow \text{erfc}\left(\sqrt{\frac{\tau}{4t}}\right),$$

$$\frac{1}{s^{1/2}}\exp(\sqrt{\tau s}) \Leftrightarrow \frac{1}{\sqrt{\pi t}}\exp\left(-\frac{\tau}{4t}\right),$$

$$\exp(\sqrt{\tau s}) \Leftrightarrow \frac{1}{t}\sqrt{\frac{\tau}{4\pi t}}\exp\left(-\frac{\tau}{4t}\right),$$

and

$$K_1(\sqrt{\tau s}) \Leftrightarrow \frac{1}{\sqrt{\tau t}}\exp\left(-\frac{\tau}{8t}\right)W_{\frac{1}{2},\frac{1}{2}}\left(\frac{\tau}{4t}\right),$$

where erfc $(x) = 1 - \text{erf}(x)$ is the complementary error function and $W_{\frac{1}{2},\frac{1}{2}}(x)$ is Whittaker's function, given by

$$W_{\frac{1}{2},\frac{1}{2}}(x) = \frac{x}{\sqrt{\pi}}\exp\left(-\frac{x}{2}\right)\int_0^\infty \exp(-x\zeta)\sqrt{\frac{\zeta + 1}{\zeta}}\,d\zeta.$$

The corresponding step response is

$$\begin{aligned}
H_\rho^S(t) = \frac{I\Delta A}{2\pi\rho^3(\tau_0 - \tau_1)}\Big[& -\tau_1\sqrt{\frac{\tau_0}{t}}\exp\left(-\frac{\tau_1}{8t}\right)W_{\frac{1}{2},\frac{1}{2}}\left(\frac{\tau_1}{4t}\right) \\
& + (\tau_0 - \tau_1 + 12t)\sqrt{\frac{\tau_0}{\pi t}}\exp\left(-\frac{\tau_0}{4t}\right) \\
& - (\tau_0 + 2\tau_1 - 12t)\,\text{erfc}\left(\sqrt{\frac{\tau_0}{4t}}\right) \\
& + (2\tau_0 - \tau_1 - 12t)\sqrt{\frac{\tau_1}{\pi t}}\exp\left(-\frac{\tau_1}{4t}\right) \\
& + (2\tau_0 + \tau_1 - 12t)\,\text{erfc}\left(\sqrt{\frac{\tau_1}{4t}}\right)\Big].
\end{aligned} \quad (20)$$

It is convenient to convert the step response to a dimensionless form. Dimensionless time x is defined as the ratio of the true time to the time constant of the upper half-space τ_0. The parameter α is the conductivity ratio σ_0/σ_1. A unit of magnetic field is the late-time step response $H_\rho^S(\infty)$, or, equivalently, the magnetic field of a static dipole given by

$$H_\rho^S(\infty) = \frac{I\Delta A}{2\pi\rho^3}. \quad (21)$$

The dimensionless step response is then

$$\frac{H_\rho^S(x)}{H_\rho^S(\infty)} = \frac{1}{\alpha - 1}\left[-\frac{1}{\sqrt{x}}\exp\left(-\frac{1}{8\alpha x}\right)W_{\frac{1}{2},\frac{1}{2}}\left(\frac{1}{4\alpha x}\right)\right.$$

$$+ (\alpha - 1 + 12\alpha x) \sqrt{\frac{1}{\pi x}} \exp\left(-\frac{1}{4x}\right)$$

$$- (\alpha + 2 - 12\alpha x) \, \text{erfc}\left(\sqrt{\frac{1}{4x}}\right)$$

$$+ (2\alpha - 1 - 12\alpha x) \sqrt{\frac{1}{\pi\alpha x}} \exp\left(-\frac{1}{4\alpha x}\right)$$

$$+ (2\alpha + 1 - 12\alpha x) \, \text{erfc}\left(\sqrt{\frac{1}{4\alpha x}}\right)\Bigg]. \qquad (22)$$

The vertical coplanar magnetic dipole-dipole (HZHZ) system

The analytical frequency response of the double half-space model to the vertical coplanar magnetic dipole-dipole system on the interface may be found in Kaufman and Keller (1983). In terms of the Laplace variable s, the frequency response is

$$H_z(s) = \frac{m(s)}{2\pi\rho^3(\tau_0 - \tau_1)s}$$

$$\times \left\{\left[9 + 9\sqrt{\tau_0 s} + 4\tau_0 s + (\sqrt{\tau_0 s})^3\right] \exp\left(-\sqrt{\tau_0 s}\right)\right.$$

$$\left. - \left[9 + 9\sqrt{\tau_1 s} + 4\tau_1 s + (\sqrt{\tau_1 s})^3\right] \exp\left(-\sqrt{\tau_1 s}\right)\right\}.$$

$$(23)$$

The step response may be found by inserting the transform of the source current found in equation (19) into equation (23) and inverting using standard integrals. In terms of true time t, the step response is

$$H_z^S(t) = \frac{9 I \Delta A}{2\pi\rho^3} \frac{t}{\tau_0 - \tau_1} \left[\left(1 - \frac{\tau_0}{18t}\right) \text{erfc}\left(\sqrt{\frac{\tau_0}{4t}}\right)\right.$$

$$+ \sqrt{\frac{\tau_0}{\pi t}}\left(1 + \frac{\tau_0}{9t}\right)\exp\left(-\frac{\tau_0}{4t}\right)$$

$$- \left(1 - \frac{\tau_1}{18t}\right)\text{erfc}\left(\sqrt{\frac{\tau_1}{4t}}\right)$$

$$\left. - \sqrt{\frac{\tau_1}{\pi t}}\left(1 + \frac{\tau_1}{9t}\right)\exp\left(-\frac{\tau_1}{4t}\right)\right]. \qquad (24)$$

The late-time step response is given by

$$H_z^S(\infty) = -\frac{I\Delta A}{4\pi\rho^3}. \qquad (25)$$

The dimensionless step response is then

$$\frac{H_z^S(x)}{H_z^S(\infty)} = \frac{18\alpha x}{\alpha - 1}\left[\left(1 - \frac{1}{18\alpha x}\right)\text{erfc}\left(\sqrt{\frac{1}{4\alpha x}}\right)\right.$$

$$+ \sqrt{\frac{1}{\pi\alpha x}}\left(1 + \frac{1}{9\alpha x}\right)\exp\left(-\frac{1}{4\alpha x}\right)$$

$$- \left(1 - \frac{1}{18x}\right)\text{erfc}\left(\sqrt{\frac{1}{4x}}\right)$$

$$- \sqrt{\frac{1}{\pi x}}\left(1 + \frac{1}{9x}\right)\exp\left(-\frac{1}{4x}\right)\Bigg]. \qquad (26)$$

This expression is exact; a large conductivity contrast is not required.

The vertical magnetic field of an electric dipole system (EPHIHZ)

Chave and Cox (1982) derive the expression for the vertical magnetic field of a horizontal electric dipole of moment $pe^{i\omega t}$ oriented azimuthally to the receiver. On the interface this expression in terms of the Laplace variable s reduces to

$$H_z(s) = \frac{2p(s)}{4\pi s(\sigma_0 - \sigma_1)} \int_0^\infty (u_0 - u_1)\lambda^2 J_1(\lambda\rho)\, d\lambda, \qquad (27)$$

which may be simplified using equation (15) to give

$$H_z(s) = \frac{p(s)}{2\pi\rho^4 s}\frac{1}{(\sigma_0 - \sigma_1)}$$

$$\times \left[(3 + 3\sqrt{\tau_1 s} + \tau_1 s)\exp\left(-\sqrt{\tau_1 s}\right)\right.$$

$$\left. - (3 + 3\sqrt{\tau_0 s} + \tau_0 s)\exp\left(-\sqrt{\tau_0 s}\right)\right]. \qquad (28)$$

A current I switched on at time $t = 0$ in a wire of length $\Delta\ell$ and held constant has the transform

$$p(s) = I\Delta\ell/s. \qquad (29)$$

The step response is then

$$H_z^S(t) = \frac{3\mu_0 I\Delta\ell}{2\pi\rho^2}\frac{t}{(\tau_0 - \tau_1)}$$

$$\times \left[\left(1 - \frac{\tau_1}{6t}\right)\text{erfc}\left(\sqrt{\frac{\tau_1}{4t}}\right) + \sqrt{\frac{\tau_1}{\pi t}}\exp\left(-\frac{\tau_1}{4t}\right)\right.$$

$$\left. - \left(1 - \frac{\tau_0}{6t}\right)\text{erfc}\left(\sqrt{\frac{\tau_0}{4t}}\right) - \sqrt{\frac{\tau_0}{\pi t}}\exp\left(-\frac{\tau_0}{4t}\right)\right]. \qquad (30)$$

The late-time response is equal to

$$H_z^S(\infty) = \frac{\mu_0 I\Delta\ell}{4\pi\rho^2}, \qquad (31)$$

so that the dimensionless step response is given by

$$\frac{H_z^S(x)}{H_z^S(\infty)} = \frac{6\alpha x}{\alpha - 1}$$

$$\times \left[\left(1 - \frac{1}{6\alpha x}\right)\text{erfc}\left(\sqrt{\frac{1}{4\alpha x}}\right) + \sqrt{\frac{1}{\pi\alpha x}}\exp\left(-\frac{1}{4\alpha x}\right)\right.$$

$$\left. - \left(1 - \frac{1}{6x}\right)\text{erfc}\left(\sqrt{\frac{1}{4x}}\right) - \sqrt{\frac{1}{\pi x}}\exp\left(-\frac{1}{4x}\right)\right]. \qquad (32)$$

As for the HZHZ case, this expression is exact.

The vertical magnetic field of a large-loop (HZHZC) system

It is worthwhile to consider a variation on the HZHZ system in which the vertical magnetic receiver is placed at the center of the source loop, denoted here as the HZHZC system. Such an apparatus has been deployed in shallow seas and moved systematically over the sea floor. It could also be mounted as a fixed-wing device on a remote-operated vehicle or a submersible. For this problem it is necessary to consider the finite dimensions of the source loop explicitly rather than using a point dipole approximation. For a loop of radius a carrying an electric current I and lying on the interface between half-spaces of conductivities σ_0 and σ_1, the frequency response in terms of the Laplace variable s for the vertical magnetic field is

$$H_z(s) = \frac{I}{a(\tau_0 - \tau_1)}\left[(\tau_1 s + 3\sqrt{\tau_1 s} + 3)\exp(-\sqrt{\tau_1 s}) \right.$$
$$\left. - (\tau_0 s + 3\sqrt{\tau_0 s} + 3)\exp(-\sqrt{\tau_0 s}) \right], \qquad (33)$$

where the time constant is defined as

$$\tau_i = \mu_0 \sigma_i a^2.$$

The step response may be found by inserting the transform of the source current I/s into equation (33) and inverting to the time domain, so that

$$H_z^S(t) = \frac{3I}{a}\frac{t}{(\tau_0 - \tau_1)}$$
$$\times \left[\left(1 - \frac{\tau_1}{6t}\right)\text{erfc}\left(\sqrt{\frac{\tau_1}{4t}}\right) + \sqrt{\frac{\tau_1}{\pi t}}\exp\left(-\frac{\tau_1}{4t}\right) \right.$$
$$\left. - \left(1 - \frac{\tau_0}{6t}\right)\text{erfc}\left(\sqrt{\frac{\tau_0}{4t}}\right) - \sqrt{\frac{\tau_0}{\pi t}}\exp\left(-\frac{\tau_0}{4t}\right) \right]. \qquad (34)$$

The late-time response is given by

$$H_z^S(\infty) = \frac{I}{2a}, \qquad (35)$$

which yields the dimensionless step response

$$\frac{H_z^S(x)}{H_z^S(\infty)} = \frac{6ax}{\alpha - 1}$$
$$\times \left[\left(1 - \frac{1}{6ax}\right)\text{erfc}\left(\sqrt{\frac{1}{4ax}}\right) + \sqrt{\frac{1}{\pi ax}}\exp\left(-\frac{1}{4ax}\right) \right.$$
$$\left. - \left(1 - \frac{1}{6x}\right)\text{erfc}\left(\sqrt{\frac{1}{4x}}\right) - \sqrt{\frac{1}{\pi x}}\exp\left(-\frac{1}{4x}\right) \right]. \qquad (36)$$

This expression is identical to that for the EPHIHZ system (although the time constant is defined differently and the late-time response is distinct).

The horizontal coaxial electric dipole-dipole (ERER) system

For completeness, we include our formula for the dimensionless step response studied by Edwards and Chave (1986) for the case $\sigma_0 \gg \sigma_1$ and used to create Figure 1. In deriving a more accurate expression, we expand equation (6) of Edwards and Chave (1986) as a power series to yield a modified form for equation (8),

$$F_{\text{TM}}(s) = -\frac{1}{\sigma_0}\frac{\partial}{\partial\rho}\int_0^\infty \left(u_0 - \frac{u_0^2 \sigma_1}{u_1 \sigma_0} + \frac{k_0^3 \sigma_1^2}{u_1^2 \sigma_0^2}\right)J_1(\lambda\rho)\,d\lambda. \qquad (37)$$

The resulting dimensionless step response is then

$$\frac{E_\rho^S(x)}{E_\rho^S(\infty)} = \frac{1}{2}\left\{ \text{erfc}\left(\sqrt{\frac{1}{4x}}\right) + \sqrt{\frac{1}{\pi x}}\exp\left(-\frac{1}{4x}\right)\right.$$
$$+ \text{erfc}\left(\sqrt{\frac{1}{4ax}}\right) + \sqrt{\frac{1}{\pi ax}}\left(1 + \frac{1}{2ax}\right)\exp\left(-\frac{1}{4ax}\right)$$
$$+ \frac{1}{a\sqrt{x}}\exp\left(-\frac{1}{8ax}\right)\left[\left(1 - \frac{1}{2ax}\right)W_{\frac{1}{2},\frac{1}{2}}\left(\frac{1}{4ax}\right)\right.$$
$$\left.\left. - \frac{1}{4ax\sqrt{\pi}}K_1\left(\frac{1}{8ax}\right)\right]\right\}. \qquad (38)$$

(Note that the dimensionless time x is defined in terms of τ_0, not τ_1 as in Edwards and Chave, 1986). For comparison, each curve has been scaled to yield a late-time amplitude of unity. In fact, due to the concentration of current in the more conductive medium, the late-time amplitude is proportional to $\sigma_0/(\sigma_0 + \sigma_1)$.

Discussion.—Dimensionless step responses for the ERER, HRHR, HZHZ, and EPHIHZ systems in the presence of a resistive sea floor are displayed in Figures 1, 3, 4, and 5 for values of the conductivity ratio α from 1 to 1 000. The responses shown in Figures 4 and 5 are from the exact analytic equations (26) and (32). Analytic equations (38) and (22) are only valid for large α; the results of computing them are shown as the dashed curves on Figures 1 and 3. These curves should be compared with the solid curves evaluated numerically from the Hankel transforms [equations (3) and (4) for the HRHR system and equations (2) and (3) in Edwards and Chave (1986) for the ERER system]. The numerical evaluation in the frequency domain was accomplished using software described by Chave (1983). The impulse response was then fitted in the frequency domain by least squares to a linear combination of basis functions consisting of single-pole responses. The inversion to the time domain was then accomplished by summing the analytic inverses of the product of this series and the Heaviside source function (Holladay, 1981; Prony, 1795). The high-contrast approximation is clearly valid for values of α exceeding 10. A true time scale is included in Figure 3 for a system operating on the sea floor ($\sigma_0 = 3.1$ S/m) with a transmitter-receiver separation of 100 m.

Only one of the three systems just described appears to be useful for estimating sea-floor conductivity, as predicted in the Introduction. Only the HRHR system responses are distinctly

different over the range of values of α. Their character is very similar to the responses of the ERER system.

The disparity between the sensitivities of the HRHR and the HZHZ systems to the sea-floor conductivity may be understood by application of Maxwell's image theory. For both systems, at times just after the transmitter is switched on until dimensionless times x of the order of .1, the upper half-space resembles a perfect conductor. As far as computation of magnetic fields in the lower half-space is concerned, the effect of the upper conductive half-space may be modeled by placing in the upper half-space a mirror image of both the transmitter current and the induced smoke ring in the lower half-space. For the HRHR system, the effect of the upper half-space is to *double* the horizontal field of the source and the smoke ring at the receiver. The response can rise for large α to as much as twice the free-space field of the transmitter.

At later dimensionless times (x greater than .1), the induced-current system in the seawater decays away, and ultimately the field falls to reach the free-space field of the transmitter dipole alone. The cause of the relative insensitivity of the
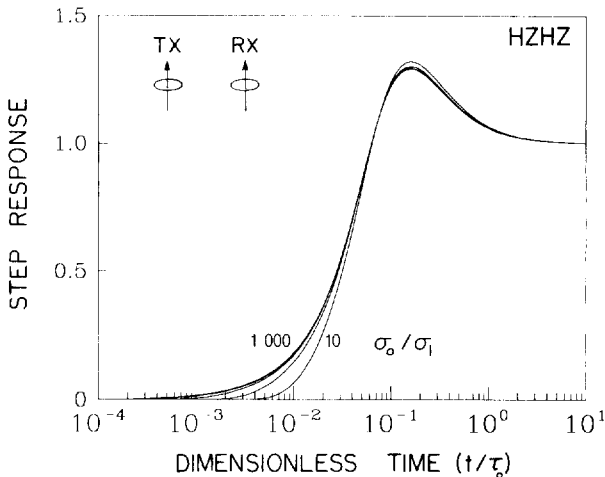

FIG. 4. The normalized step-on response for the coplanar magnetic dipole-dipole system (HZHZ) computed analytically from equation (26).
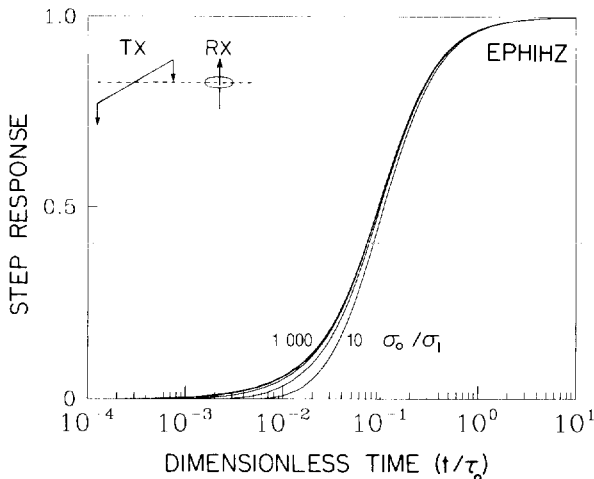

FIG. 5. The normalized step-on response for the system formed of a vertical magnetic dipole and a horizontal electric dipole (EPHIHZ) computed analytically from equation (32).

HZHZ system should now be clear. At early times, the images in the upper half-space of the transmitter current and the induced-current smoke ring in the lower half-space oppose each other. No vertical field is measured in the receiver until the seawater no longer behaves as a perfect conductor.

The transient response for a conductive sea floor

The results in Figures 1 and 3–5 are based on models where seawater is more conductive than basement rock or sediment, as is usually the case. However, there are instances in which the reverse situation might be expected, at least locally. For example, the massive polymetallic sulfide deposits discovered in conjunction with midocean ridge hydrothermal systems (e.g., Rona, 1983) are of an unprecedented concentration and could be more conductive than seawater. Transient EM systems might also find application near large metallic objects, including nonmagnetic materials, lying on the sea floor.

The expressions for the HZHZ and EPHIHZ responses in equations (26) and (32) are exact and hold for values of α smaller than 1. The TM mode parts of the HRHR and ERER responses must be rederived for the case where the conductivity σ_1 of the lower half-space exceeds that of the upper half-space σ_0. It is not difficult to show that the frequency-domain equation (17) and the time-domain equation (20) for the HRHR system are modified only by interchanging k_0 and k_1 or τ_0 and τ_1. The late-time response (21) does not depend upon the conductivity, so that the dimensionless step response corresponding to expression (22) may be written

$$
\frac{H_\rho^S(x)}{H_\rho^S(\infty)} = \frac{1}{1-\alpha}\left[-\sqrt{\frac{\alpha}{x}}\exp\left(-\frac{1}{8x}\right)W_{\frac{1}{2},\frac{1}{2}}\left(\frac{1}{4x}\right)\right.
$$
$$
+ (1-\alpha+12\alpha x)\sqrt{\frac{1}{\pi\alpha x}}\exp\left(-\frac{1}{4\alpha x}\right)
$$
$$
- (1+2\alpha-12\alpha x)\,\mathrm{erfc}\left(\sqrt{\frac{1}{4\alpha x}}\right)
$$
$$
+ (2-\alpha-12\alpha x)\sqrt{\frac{1}{\pi x}}\exp\left(-\frac{1}{4x}\right)
$$
$$
\left.+ (2+\alpha-12\alpha x)\,\mathrm{erfc}\left(\sqrt{\frac{1}{4x}}\right)\right]. \tag{39}
$$

The ERER system response for a conductive sea floor is determined in an analogous manner by interchanging k_0 and k_1 in the frequency-domain equation (37). The expression, scaled to give a late-time amplitude of unity, is

$$
\frac{E_\rho^S(x)}{E_\rho^S(\infty)} = \frac{1}{2}\left\{\mathrm{erfc}\left(\sqrt{\frac{1}{4\alpha x}}\right) + \sqrt{\frac{1}{\pi\alpha x}}\exp\left(-\frac{1}{4\alpha x}\right)\right.
$$
$$
+ \mathrm{erfc}\left(\sqrt{\frac{1}{4x}}\right) + \sqrt{\frac{1}{\pi x}}\left(1+\frac{1}{2x}\right)\exp\left(-\frac{1}{4x}\right)
$$
$$
+ \frac{\alpha}{\sqrt{x}}\exp\left(-\frac{1}{8x}\right)\left[\left(1-\frac{1}{2x}\right)W_{\frac{1}{2},\frac{1}{2}}\left(\frac{1}{4x}\right)\right.
$$
$$
\left.\left.-\frac{1}{4x\sqrt{\pi}}K_1\left(\frac{1}{8x}\right)\right]\right\}. \tag{40}
$$

Figures 6 through 9 show the ERER response (40), the HRHR response (39), the HZHZ response (26), and the EPHIHZ response (32) for values of the conductivity ratio α ranging from 0.001 to 1. In contrast to the resistive sea-floor models in Figures 1 and 3–5, the HZHZ and EPHIHZ systems are quite useful for inferring the conductivity of a relatively conductive sea floor; even when the contrast α is small, the time difference from a whole-space response is substantial. The ERER system becomes less useful as a transient system for very small values of α because the amplitude is diminished. The reason is clear: electric currents are concentrated where the conductivity is largest, resulting in small electric fields in the relatively resistive seawater. The late-time amplitude might prove a better discriminator of sea-floor conductivity for small values of α, provided that the electric field can still be detected.

The HRHR system remains useful in the conductive sea-floor limit, as seen in Figure 7. However, the size of the time separation from the whole-space response is quite small unless the ratio of conductivities α is below 0.1. This suggests that the HZHZ system or EPHIHZ system would be a more practical choice when a conductive target is sought. The relative arrival times of the two disturbances are such that the portion from the seawater always arrives first at a dimensionless time of about 1, followed by the sea-floor contribution.

THE RESPONSE OF THE HRHR SYSTEM TO OTHER STRUCTURES

The transient response of the HRHR system has been shown to consist of two parts. When the sea floor is less conductive than seawater, the form of the response at early time is dictated principally by the electrical conductivity of the sea floor, where the seawater may be regarded as a perfect conductor. The form of the response at late time is then determined by the conductivity of the seawater, with the sea floor considered as a perfect insulator. Any given response can be constructed approximately by superposition of the early-time and late-time effects. Because the late-time effect is essentially independent of the conductivity of the sea floor, the response
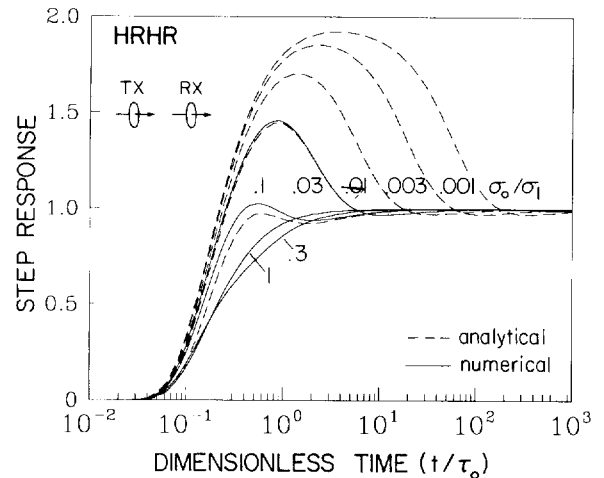

FIG. 7. The normalized step-on response for the coaxial magnetic dipole-dipole system (HRHR) for a conductive basement computed analytically from equation (39) and numerically from the frequency-domain equations (3) and (4).
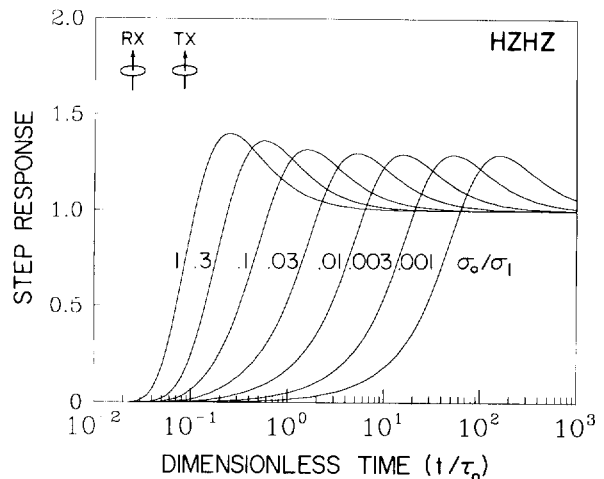

FIG. 8. The normalized step-on response for a conductive basement for the coplanar magnetic dipole-dipole system (HZHZ) computed analytically from equation (26).
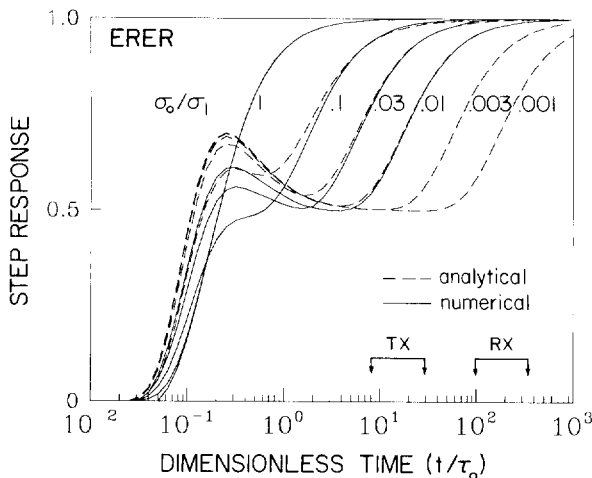

FIG. 6. The normalized step-on response for the coaxial electric dipole-dipole system (ERER) for a conductive basement evaluated analytically from equation (40) and numerically from the frequency-domain expressions given in Edwards and Chave (1986). The curves for α = 1 and α = .3 are virtually coincident.
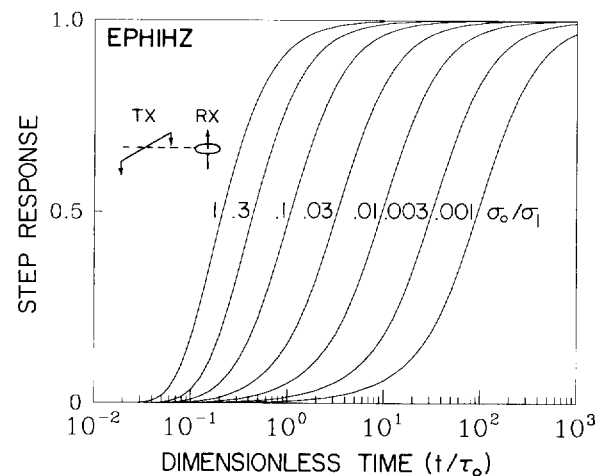

FIG. 9. The normalized step-on response for a conductive basement for the system formed of a vertical magnetic dipole and a horizontal electric dipole (EPHIHZ) computed analytically from equation (32).

of different crustal models may be simply compared by plotting only early-time responses. The result is a reduction in the number of curves necessary to illustrate the salient physics.

Layered-earth responses

Any given layered-earth response of the HRHR system may be calculated numerically from equations (3) and (4) by inserting the appropriate reflection coefficients for the PM and TM modes, R_{PM} and R_{TM}. These coefficients are computed using the recursion relationships given in Dey and Ward (1970), or the continued-fraction expansions of Chave and Cox (1982).

The models considered are a crustal layer over a very resistive half-space (Figure 10), a crustal half-space containing a thin, very resistive zone (Figure 11), and a crustal layer over a very conductive half-space (Figure 12). In each case, the upper half-space representing the sea is assumed to be perfectly conductive. For these three cases, equations (3) and (4) have the following forms.

The resistive basement

$$F_{PM}(s) = \frac{m(s)}{4\pi} \int_0^\infty 2u_1 \left[\frac{A(s) - 1}{A(s) + 1} \right] \left[\lambda J_0(\lambda\rho) - \frac{1}{\rho} J_1(\lambda\rho) \right] d\lambda,$$
(41)

and

$$F_{TM}(s) = \frac{-2k_1^2 m(s)}{4\pi\rho} \int_0^\infty \frac{J_1(\lambda\rho)}{u_1} \left[\frac{1 - \exp(-2u_1 d)}{1 + \exp(-2u_1 d)} \right] d\lambda,$$
(42)

where

$$A(s) = \frac{u_1 - \lambda}{u_1 + \lambda} \exp(-2u_1 d),$$

and d is the depth to the basement.

The thin resistive zone

$$F_{PM}(s) = \frac{-2m(s)}{4\pi} \int_0^\infty u_1 \left[\lambda J_0(\lambda\rho) - \frac{1}{\rho} J_1(\lambda\rho) \right] d\lambda,$$
(43)

and

$$F_{TM}(s) = \frac{-2k_1^2 m(s)}{4\pi\rho} \int_0^\infty \frac{J_1(\lambda\rho)}{u_1} \left[\frac{1 - \exp(-2u_1 d)}{1 + \exp(-2u_1 d)} \right] d\lambda,$$
(44)

and d is the depth to the thin resistive layer.

The perfectly conductive basement

$$F_{PM}(s) = \frac{m(s)}{4\pi} \int_0^\infty 2u_1 \left[\frac{1 + \exp(-2u_1 d)}{1 - \exp(-2u_1 d)} \right]$$

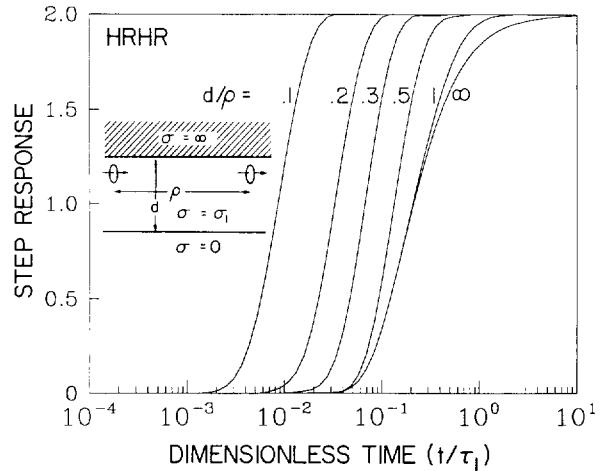$$\times \left[\lambda J_0(\lambda\rho) - \frac{1}{\rho} J_1(\lambda\rho) \right] d\lambda,$$
(45)

FIG. 10. The step-on response of the double half-space model modified by the inclusion of a resistive basement at a depth d to the HRHR system for a range of values of the normalized layer thickness d/ρ.
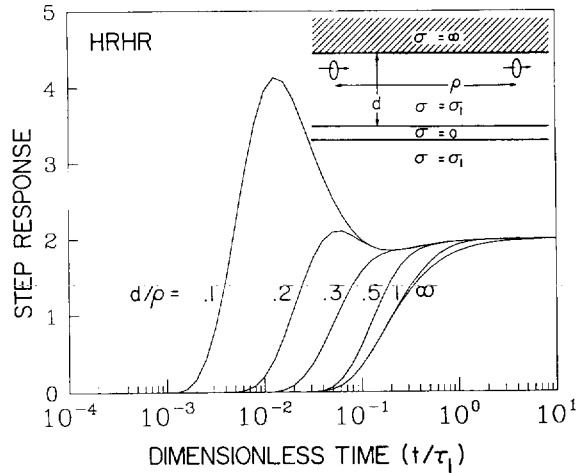

FIG. 11. The step-on response of the double half-space model modified by the inclusion of a very thin, resistive zone at a depth d to the HRHR system for a range of values of the normalized depth to the resistive zone d/ρ.
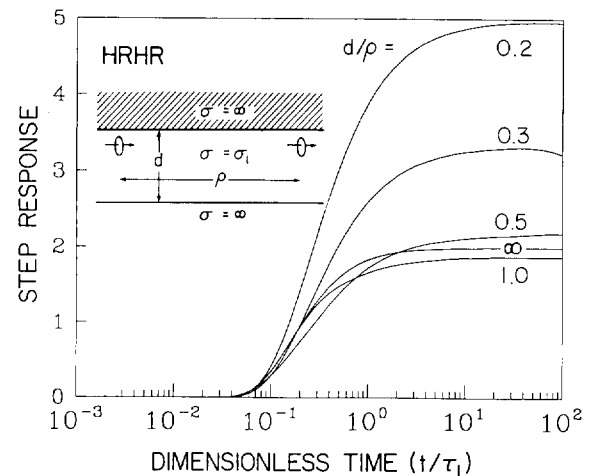

FIG. 12. The step-on response of the double half-space model modified by the inclusion of a conductive basement at a depth d to the HRHR system for a range of values of the normalized layer thickness d/ρ.

and

$$F_{TM}(s) = \frac{-2k_1^2 m(s)}{4\pi\rho} \int_0^\infty \frac{J_1(\lambda\rho)}{u_1} \left[\frac{1 + \exp(-2u_1 d)}{1 - \exp(-2u_1 d)} \right] d\lambda,$$

(46)

where d is the depth to the basement.

Equations (41) to (46) were evaluated numerically in the same manner as for the step responses of the ERER and HRHR systems. The step responses for the three models stated above are plotted in Figures 10, 11, and 12. Time normalization is with respect to τ_1, the characteristic diffusion time in the crustal layer, and not τ_0 as in earlier figures. The response of a crustal half-space alone corresponds in each of the figures with the case where the depth d is infinite.

The presence of the resistive basement shifts the half-space response to earlier time. The amount of shift is a strong function of the depth to the basement; the smaller the depth, the larger the shift. The relatively resistive basement provides a faster path for the signal to reach the receiver, so that the signal arrives earlier than it might were there no basement. The effect can be compared with that of a refracted wave in seismology, where an acoustic wave, because it enters a higher velocity layer, arrives at a receiver ahead of the direct wave. The shift is minimal for depths to the basement exceeding one-half the transmitter-receiver separation ρ. We may deduce that the depth of investigation of the HRHR system in this environment is on the order of $\rho/2$.

The resistive zone is at first sight a somewhat unrealistic model physically but it could represent, for example, a thin layer of permafrost in an otherwise conductive sea floor. To the PM mode of propagation, the model is transparent since the horizontal current flow associated with this mode is not perturbed by the zone. The contribution (43) to the magnetic field is just the expression for the field of a uniform half-space beneath the sea. The TM mode is affected because the vertical currents associated with it cannot pass through the resistive zone. The TM mode fields of both the thin layer and the resistive basement are the same, so that equation (44) is identical to equation (42). The family of responses of resistive zones located at a range of depth values is plotted in Figure 11. Surprisingly, the effect of a thin layer is very much stronger than that of a resistive half-space. In the model of a resistive basement, the shape of the transient remains virtually the same for different values of d when plotted logarithmically. In the model of a resistive zone, the shape changes markedly and may be of a much larger amplitude. For instance, for $d/\rho = .1$, the amplitude of the transient signal is more than four times the amplitude of the free-space field.

The response for the conductive basement is plotted in Figure 12. As the thickness of the layer is reduced, the signal amplitude increases and asymptotically approaches a value greater than 2. This occurs because the images of the transmitter current in what are now two very good conductors form an infinite series with a sum which can be much more than twice the free-space field of the transmitter alone. As the thickness of the layer decreases, the images become more closely spaced; and the combined effect increases at a rate inversely proportional to the thickness of the layer. The arrival time does not appear to be markedly influenced by the depth to the layer, presumably because the smoke ring diffuses only through the layer of finite conductivity.

Three-dimensional models

The modeling of a large range of 3-D bodies contained in the sea floor is simplified greatly by assuming that the sea layer behaves as a perfect conductor at early times. The simplifying theorem follows directly from the discussion of images. When a magnetic dipole transmitter is located on the boundary between a perfect conductor and a lower half-space containing an arbitrary conductivity distribution, the field measured anywhere in the half-space is identical to that which would be produced by a transmitter of twice the moment if the conductivity distribution of the lower half-space were mirror imaged in the perfect conductor. This theorem is par-
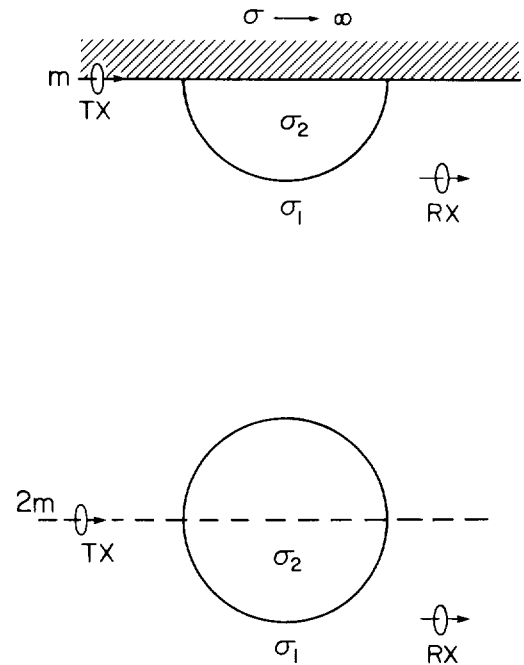

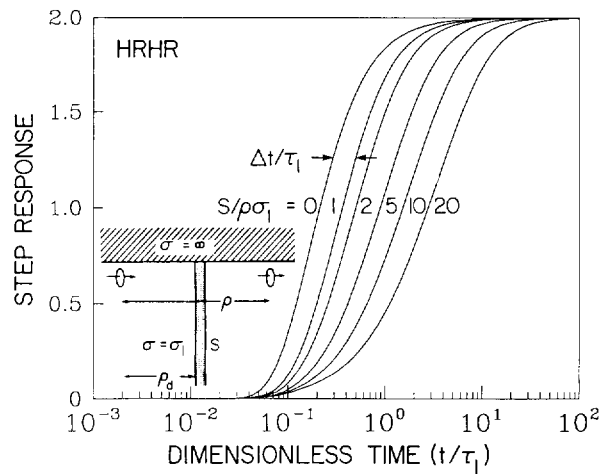FIG. 13. A semibody problem and its equivalent whole-space representation.

FIG. 14. The transient step-on response of the double half-space model modified by the inclusion of a semiinfinite vertical dike with conductance S situated at a distance ρ_d from the transmitter to the HRHR system for a range of values of the normalized dike conductance $S/\rho\sigma_1$.

ticularly useful for calculating the response of a semibody, for example, a hemisphere. When the image of the hemisphere is added to the hemisphere itself, the whole becomes a sphere and the response of a sphere *in a whole space* is readily found.

The theorem is illustrated in Figure 13, where a transmitter of moment *m* interacting with a hemisphere touching the interface is replaced by a transmitter of moment 2*m* interacting with a sphere in a whole space. The proof is trivial and consists of showing that the boundary conditions at the interface associated with the two models are identical. At the boundary with the perfect conductor, the tangential electric field and the vertical magnetic field must vanish. In the whole-space model, both of these conditions are met by symmetry. Doubling of the transmitter strength is demanded by the method of images.

We discuss only one application of the semibody theorem. The response characteristics of the HRHR system to a finite vertical conductive dike shown in Figure 14 is computed. Application of the theorem indicates that an equivalent problem is computation of the transient response of an infinite sheet in a whole space to a magnetic dipole source whose axis is perpendicular to the sheet. The receiver is coaxial with the receiver. The transmitter is at the origin and the receiver is a distance ρ away. A vertical dike of conductance S is located at ρ_d. The normalized frequency response is described by two expressions, depending upon whether ρ_d is less than or greater than ρ. If $\rho_d < \rho$,

$$\frac{H_\rho(s)}{H_\rho(\infty)} = \frac{\rho^3}{2} \int_0^\infty \frac{\lambda^3}{u_1} \left[\frac{\theta(s)}{1 + \theta(s)} \right] \exp\left(-u_1 \rho \right) d\lambda, \quad (47)$$

whereas if $\rho_d > \rho$,

$$\frac{H_\rho(s)}{H_\rho(\infty)} = \frac{\rho^3}{2} \int_0^\infty \frac{\lambda^3}{u_1} \left[\frac{\theta(s)}{1 + \theta(s)} \right] \exp\left[-u_1(2\rho_d - \rho) \right] d\lambda, \quad (48)$$

where

$$\theta(s) = \frac{s\mu_0 S}{2u_1}.$$

If the dike is between the transmitter and receiver, the response is not sensitive to the particular position of the dike,
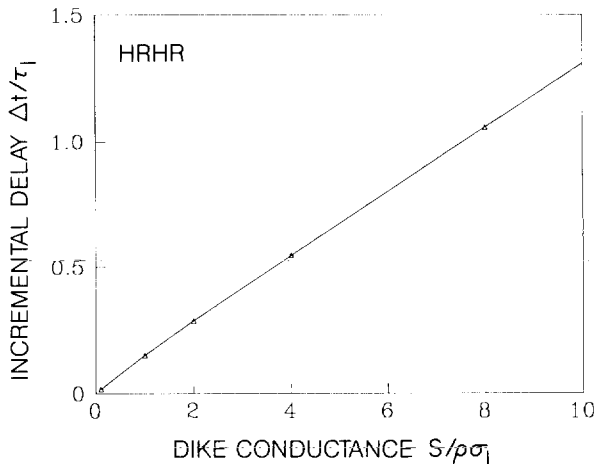

FIG. 15. The incremental delay time $\Delta t/\tau_1$ obtained from Figure 14 as a function of the normalized dike conductance.

but only to the transmitter-receiver separation. The presence of the dike serves to delay the arrival of the signal at the receiver, with the amount of delay being determined by the specific conductance of the dike, as illustrated in Figure 14, for a range of values of a normalized form of the dike conductance. The plot of the incremental delay versus the dike conductance shown in Figure 15 indicates a nearly linear relationship between them.

ESTIMATES OF TWO SYSTEMATIC ERRORS ASSOCIATED WITH A TOWED HRHR SYSTEM

Some of the important requirements of a practical system can be studied theoretically. For example, the system should be relatively immune to small errors in positioning and orientation. In order to determine to some measure the robustness of the horizontal magnetic dipole system, the effects of two such errors are investigated.

We envisage that a practical system should be resting on the ocean floor whenever measurements are made in order to minimize the noise caused by the movement of the array through the Earth's magnetic field. Nevertheless the transmitter and receiver cannot be positioned exactly at the boundary, because shallow layers of sediment may cover the basement rock and may differ little in conductivity from the seawater, and because the axes of the transmitter and receiver must of necessity be raised above the sea floor because of their finite size. The consequences may be investigated by raising the receiver a small distance and noting the effect on the transient response. This is accomplished through upward continuation of the field computed on the boundary. A number of cases were studied, and the example, in which the receiver is raised off the ocean floor by a distance equal to 2 percent of the array separation, is shown in Figure 16. In terms of a real distance, 2 percent might represent 2 m for a design separation of 100 m. A comparison between the dashed curves, which represent the fields on the boundary, and the solid curves, which represent the upward continued fields, reveals that the effect of elevating the receiver is to introduce a delay in the received step response, because the signal must travel an extra short distance through a conductive medium. The effect becomes more important for greater conductivity contrasts because the diffusion time through the sea amounts to a significant portion of the entire diffusion time. The incremental delay time due to the extra signal path length is not solely dependent on the conductivity of the sea but is also dependent on the sea floor conductivity. The amount of delay actually decreases with greater conductivity contrasts, but the fractional increase becomes more significant. Fortunately, the effect remains small for typical conductivity ratios up to a value of 30.

The effect of the misalignment of the transmitter may be determined by examining the two worst-case scenarios of misorientation. In the first case the axis of the transmitter remains horizontal but is rotated by 90 degrees to form an HPHIHR system. It is not difficult to see by symmetry that any magnetic field at the receiver must be perpendicular to the receiver axis, so that no signal is ever detected. The only error introduced by the horizontal misorientation of a real system would be due to a cosine type variation of the HRHR component of the signal. In the second case the transmitter axis is rotated by 90 degrees to the vertical, forming an HZHR system. Kaufman

and Keller (1983) have derived the expression for the radial magnetic field of a vertical magnetic dipole. The form of their expression in terms of the Laplace variable s is

$$H_\rho(s) = \frac{m(s)}{4\pi\rho^3}(\tau_0 - \tau_1)s$$

$$\times \left[I_2(a\sqrt{s})K_2(b\sqrt{s}) - \frac{\alpha + 1}{\alpha - 1} I_1(a\sqrt{s})K_1(b\sqrt{s}) \right], \quad (49)$$

where

$$a = \frac{\sqrt{\tau_0} - \sqrt{\tau_1}}{2},$$

and

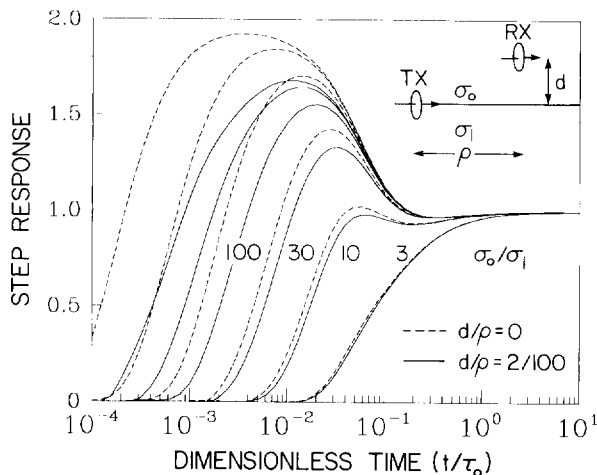$$b = \frac{\sqrt{\tau_0} + \sqrt{\tau_1}}{2},$$

FIG. 16. The normalized step-on response of the HRHR system when the receiver is raised a distance $d/\rho = .02$ off the interface (solid line) is compared to the response when both transmitter and receiver are on the boundary (dashed lines).
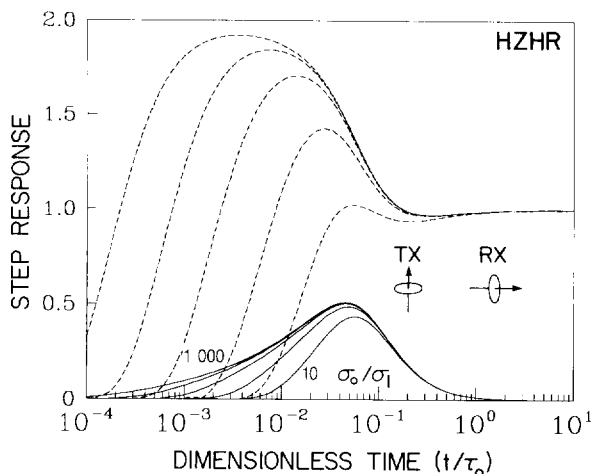

FIG. 17. The normalized step-on response for the null-coupled (HZHR) system computed analytically from equation (51) for a range of values of the conductivity ratio α (solid lines). The HRHR response shown in Figure 3 is included for comparison (dashed lines).

and where I_v and K_v are modified Bessel functions. The step response, plotted in Figure 17, is then

$$H_\rho^S(t) = \frac{I\Delta A}{4\pi\rho^3} \frac{(\tau_0 - \tau_1)}{2t} \exp\left(-\frac{\tau_0 + \tau_1}{8t}\right)$$

$$\times \left[I_2\left(\frac{\tau_0 - \tau_1}{8t}\right) - \frac{\alpha + 1}{\alpha - 1} I_1\left(\frac{\tau_0 - \tau_1}{8t}\right) \right]. \quad (50)$$

The HZHR system is null coupled. The measured component tends to zero at late times, so that it is not possible to normalize equation (50) through division by $H_\rho(\infty)$. However, if the late-time response of the HRHR system is used, the resulting expression may be directly compared with equation (22) to determine the significance of an error in orientation. The final dimensionless expression is then

$$\frac{H_\rho^S(x)}{H_\rho^S(\infty)} = \frac{(\alpha - 1)}{4\alpha x} \exp\left(-\frac{\alpha + 1}{8\alpha x}\right)$$

$$\times \left[I_2\left(\frac{\alpha - 1}{8\alpha x}\right) - \frac{\alpha + 1}{\alpha - 1} I_1\left(\frac{\alpha - 1}{8\alpha x}\right) \right]. \quad (51)$$

In Figure 17 the dashed and solid curves represent, respectively, the responses of the HRHR and HZHR systems. By reciprocity, the HZHR system represents the largest cross-coupling error which may be introduced by the misalignment of either the transmitter or the receiver. The cross-coupled component never exceeds 50 percent of the proper signal, and for most times and conductivity ratios it is much smaller. In an actual case of misalignment the cross-coupled component of the transmitter field would be weighted by the sine of the misalignment angle, and the in-line component by the cosine of the misalignment angle. It is likely that this angle would be quite small, of the order of a few degrees; consequently, errors associated with the introduction of a cross-coupled component should be small.

CONCLUSIONS

Our study of some of the possible configurations for a transient, sea-floor electromagnetic system reveals that two systems, the ERER and HRHR systems, are well suited to the determination of sea-floor conductivity if the sea floor is less conductive than the seawater. The diagnostic characteristic common to these two systems is the almost instantaneous response they have to a step-on current when used on land, at the boundary between a conductive and a dielectric half-space. If the dielectric is replaced by a relatively weak conductor, in this discussion the sea floor, the instantaneous response is broadened and delayed. Moreover, for conductivity ratios larger than about ten, it is separated in time from the part of the response which changes when the conductivity of the seawater changes. Put another way, the location in time of the initial rise in the transient response provides a direct means of determining the apparent conductivity of the sea floor, while the character of the signal at later times may be inverted only for the seawater conductivity.

An analytic solution for the step-on response of the HRHR system at the boundary of two adjoining half-spaces has been derived. It is valid for all time, and for conductivity ratios greater than about ten, and it has been used to confirm the accuracy of the numerical evaluations of the closed-form solutions.

In the less common instance where the target is more conductive than seawater, we have shown that the HZHZ, EPHIHZ, and HZHZC systems are useful for the determination of electrical conductivity. In all cases, the portion of the transient traveling in seawater arrives first, and the time separation between it and the final part due to propagation in rock is a measure of the apparent conductivity. The ERER system suffers from a decrease in signal amplitude when the target is highly conductive. This suggests that a practical sea-floor transient EM system might incorporate a combination of the HRHR and HZHZ or HZHZC types to yield the maximum sensitivity to structure.

The separation in time of the HRHR response into sea floor and seawater parts enables the relevant, early-time behavior of a number of models to be computed simply, using the approximation that the upper, sea layer is perfectly conductive. The responses of the system to three-layered earth models (basically a uniform half-space with one additional feature, namely a resistive basement, a resistive zone, or a conductive basement) are radically different and, in particular, the response of a thin, resistive zone in a crustal half-space differs substantially from the response of the half-space alone. The latter result demonstrates a fundamental difference in the induced current modes for the sea floor and land environments. The effect of a vertical, infinite, conductive dike, outcropping at the sea floor, is shown to produce a delay in the initial transient response. The delay as an increment from the delay caused by the crustal layer alone varies linearly with dike conductance. This suggests that time delay could be inverted directly to give some measure of the anomalous integrated conductivity of the sea floor which lies both between and in the vicinity of the transmitter and the receiver.

The design of any practical HRHR system requires solution of a number of theoretical problems, two of which were addressed here. It was shown that the effect of misalignment is negligible, whereas a displacement of the system off the sea floor could lead to substantial errors in interpretation, especially for cases of high conductivity contrast between seawater and sea floor.

ACKNOWLEDGMENTS

REFERENCES

Ballard, R. D., and Francheteau, J., 1982, The relationship between active sulphide deposition and the axial processes of the Mid-Ocean Ridge: Mar. Tech. Soc. J., **16**, 8–22.
Bannister, P. R., 1968, Determination of the electrical conductivity of the sea bed in shallow waters: Geophysics, **33**, 995–1003.
Chave, A. D., 1983, Numerical integration of related Hankel transforms by quadrature and continued fraction expansion: Geophysics, **48**, 1671–1686.
——— The Frechet derivatives of electromagnetic induction: J. Geophys. Res., **89**, 3373–3380.
Chave, A. D., and Cox, C. S., 1982, Controlled electromagnetic sources for measuring electrical conductivity beneath the oceans—1. Forward problem and model study: J. Geophys. Res., **87**, 5327–5338.
Coggon, J. H., and Morrison, H. F., 1970, Electromagnetic investigation of the sea floor: Geophysics, **35**, 476–489.
Dey, A., and Ward, S. H., 1970, Inductive sounding of a layered earth with a horizontal magnetic dipole: Geophysics, **35**, 660–703.
Edwards, R. N., and Chave, A. D., 1986, On the theory of a transient electric dipole-dipole method for mapping the conductivity of the sea floor: Geophysics, **51**, 984–987.
Edwards, R. N., Law, L. K., and Delaurier, J. M., 1981, On measuring the electrical conductivity of the oceanic crust by a modified magnetometric resistivity method: J. Geophys. Res., **86**, 11609–11615.
Hekinian, R., Fevrier, M., Bischoff, J. C., Picot, P., and Shanks, W. C., 1980, Sulfur deposits from the East Pacific Rise near 21°N: Science, **207**, 1433–1444.
Hohmann, G. W., and Ward, S. H., 1986, Electromagnetic theory for geophysical applications: in Nabighian, M. N., Ed.: Soc. Explor. Geophys.
Holladay, J. S., 1981, YVESFT and CHANNEL: A subroutine package for stable transformation of sparse frequency domain electromagnetic data to the time domain: Res. Appl. Geophys., **17**, Univ. of Toronto.
Kaufman, A. A., and Keller, G. V., 1983, Frequency and transient soundings: Amsterdam, Elsevier Science Publ. Co., 411–450.
Malahoff, A., 1982, A comparison of the massive submarine polymetallic sulfides of the Galapagos Rift with some continental deposits: Marine Tech. Soc. J., **16**, 39–45.
Nabighian, M. N., 1979, Quasi-static transient response of a conducting half-space—An approximate representation: Geophysics, **44**, 1700–1705.
Nobes, D. C., Villinger, H., Davis, E. E., and Law, L. K., 1986, Estimation of oceanic sediment bulk physical properties at depth from sea floor geophysical measurements: J. Geophysical Res., in press.
Normark, W. R., Morton, J. C., Koski, R. A., Clague, D. A., and Delancy, J. R., 1983, Active hydrothermal vents and sulfide deposits on the southern Juan de Fuca ridge: Geology, **11**, 158–163.
Prony, R., 1795, Essai experimental et analytique sur les lois de la dilatabilite des fluides elastiques et sur celles de la force expansive de la vapeur de l'alcool a differentes temperatures: J. l'Ecole Polytech., Paris, **1**, 24–76.
Rona, P. A., 1983, Exploration for hydrothermal mineral deposits at sea floor spreading centers: Mar. Mining, **4**, 7–38.
Spies, B., and Frischknecht, F. C., 1986, Electromagnetic sounding, in Nabighian, M. N., Ed.: Soc. Explor. Geophys.
Watson, G. N., 1966, A treatise on the theory of Bessel functions: Cambridge Univ. Press., 2nd ed., 425.